Numerical simulation of the electromagnetic decay of the nuclei $^{152-154-156}$Dy with selfconsistent collective Strength Functions.

V. Martin
Análisis Numérico, Facultad de Informática
Universidad Politécnica de Madrid
E-28660 Madrid, Spain.

J.L. Egido
Departamento de Física Teórica C-XI
Universidad Autónoma de Madrid
E-28049 Madrid, Spain.

T. L. Khoo and T. Lauritsen
Argonne National Laboratory, Argonne, Illinois, USA
(November 11, 1993)

Abstract

The electromagnetic decay of the nuclei $^{152-154-156}$Dy is analyzed using microscopic Hartree-Fock calculations at finite temperature. The theoretical collective transition probabilities are implemented in numerical simulations to produce theoretical espectra. Thermal shape fluctuations are also taken into account. The inclusion of these correlation is crucial in order to understand the main features of the collective $E2$ spectra of these isotopes at different energies. The theoretical calculations suggest a shape change as responsible for the unusual features of the spectrum of the nucleus ^{154}Dy at high energy.

21.10.Re 21.10Ky

Typeset using REVTEX

I. INTRODUCTION

In the last years much progress has been made in the understanding of nuclear structure problems in the high spin region of heavy nuclei. Most of these studies have been devoted to the yrast region where many new phenomena have been discovered through the study of discrete lines. Some investigations have been made of states excited up to 8 MeV above the yrast line using quasicontinuum γ rays. This region is very interesting because new physics is expected to be found there, for example, damping of the rotational motion, pairing phase transitions and shape changes.

The description of the quasicontinuum is difficult not only experimentally but also theoretically. On the theoretical side any kind of microscopic description of the quasicontinuum is very complicated because of the high level density that characterizes this region. It is obvious that a microcanonical description is impossible, besides the fact that no one is interested in the detailed properties of each level. On the other hand, from the experience with the discrete states we have learned that a selfconsistent mean field approximation is a very convenient way to start with. As a matter of fact much progress has been made within the Hartree Fock Bogoliubov (HFB) theory and its cranked version (CHFB approximation) [1,2]. The key point for the success of the mean field approximation is based in the fact that many correlations are taken into account by allowing symmetry breaking wave functions in the variational ansatz. The direct generalization of this theory to high excitation energy uses the grand canonical ensemble combined with the mean field approximation, i.e. the finite temperature HFB (FTHFB) [3–5]. In this theory one has been able to describe most of the observed phenomena at high spin and high excitation energies. The limitations of the mean field approximation at finite temperature do have the same origin as at zero temperature: the lack of correlations. While at zero temperature (T) only the quantum fluctuations are missing, at finite temperature one also has to consider the thermal fluctuations. At finite T it seems that the more important fluctuations around the mean values are those of thermal origin. This is fortunate because these can be taken into account in a rather straightforward way [6–8] by statistical averaging around the mean values.

A definite prediction of the FTHFB theory is that a phase transition occurs either with increasing temperature at fixed spin or with increasing spin at fixed temperature [9,10]. The phases correspond to collective motion on one hand and aligned-particle motion ($\gamma = -60°$ in our convention) on the other hand. This prediction has been also made using the Landau theory of phase transitions [11,12]. On a plot of energy vs. spin, a characteristic phase diagram is obtained (see for example Fig. 3 of [13]). In a finite system, where the phase transition may be smeared out by fluctuations, it is an interesting general problem in mesoscopic physics to explore the remnant signatures of the phase transitions. This is the central problem we wish to address in this paper.

Recent experiments on a sequence of Dy isotopes with mass 152, 154 and 156 [14,15] have extracted the quasicontinuum E2 spectra arising from excited γ cascades. All three nuclei displayed a pronounced collective E2 component, usually in the form of a broad peak. However, an unexpected splitting into two distinct parts was observed only in ^{154}Dy, which clearly implied a structural change along the γ cascade. This unusual splitting may well be a signature for a shape phase transition. We shall explore this possibility in this paper by investigating whether the splitting is related to a phase transition predicted in the mean field

theory. The structure properties of these nuclei have been analyzed in the preceding paper [13], they have been studied within the FTHFB and with inclusion of shape fluctuations. We refer the interested reader to it for a detailed study.

The purpose of this paper is to calculate the quasicontinuum E2 spectra in the above-mentioned Dy isotope, using the results of (a) mean field theory (FTHF) and (b) with the additional inclusion of fluctuations. Two particular points of interest are (i) the role of fluctuations, e.g. in generating an E2 peak in ^{152}Dy [14] where none is expected is expected on the basis of the FTHFB and (ii) whether a phase transition can give rise to observable signatures, e.g. the two separate E2 components observed in ^{154}Dy [15].

It should be pointed out that it is a very demanding task to obtain a theoretical spectrum which reproduces the measured ones. This would require an excellent theoretical description of the collective properties as a function of spin and excitation energy (up to $\sim$ 8 MeV). Earlier work [10,16,17] have attempted to explain the features of the E2 quasicontinuum γ-rays in transitional nuclei. Goodman [10,16] used calculated properties of ^{158}Yb, the isotone of ^{154}Dy, to explain spectral features of the latter. Alhassid and Bush [17] studied the spectra of ^{152,154,156}Dy in the framework of the Landau theory. In both cases, only average properties along the average decay pathways found in ref. [15] were calculated. The improvement in the present work is that actual spectra are calculated from cascades codes where theoretical $B(E2)$ values were implemented. The starting point was an entry distribution with no restriction to an average pathway.

The paper is organized as follows. In sect. 2 the underlying theory is examined. In sect. 3 the numerical simulation of the γ cascade is described. Sect. 4 and 5 report the results of the simulation and the conclusions.

II. THEORY

For all the investigations corresponding to the decay of hot nuclei the background of statistical γ-rays plays a crucial role. In the analysis of nearly all the experiments for this purpose one has used the statistical model. See ref. [18] for a recent review on the electromagnetic decay of a hot nucleus. Calculations based on simple models [19–21] unfortunately carry considerable uncertainties. In the statistical model, for instance, the energy dependence of the level density is crucial but only poorly known. The same applies to the ratio of average M1, E1 and E2 matrix elements [21]. In the statistical model the M1 and E2 matrix elements are taken constant, and the E1 has an energy dependence to take into account the strength of the giant dipole resonance. On the other hand, an exact calculation, taking into account the decay properties of all states with spin $I\hbar$ in the energy interval between E and $E + \mathrm{d}E$, is clearly out of the question in the continuum region.

An alternative microscopic method to calculate the transition rates has been developed in [22] and [23]. There the random-phase approximation (RPA) is combined with the finite-temperature (FT) cranked Hartree-Fock-Bogoliubov (CHFB) approach in the formalism of the grand canonical ensemble. This is done first by solving the FTCHFB equations for given values of cranking frequency and temperature. Small oscillations around the minima so determined are subsequently taken into account in terms of the FTRPA.

The HFB approximation has been used in nearly all microscopic investigations of states near the yrast line [1,2], where it works very well. The extension to finite temperatures

likewise has been very successful [3–5]. In principle, this approximation provides the information necessary to calculate transition strengths as functions of (E, I). The use of the grand canonical ensemble is justified because the level density is very high already 1 or 2 MeV above the yrast line. In general one should add the RPA for two reasons. First it shifts the collective strengths of the low-lying vibrations and the giant resonances to their proper places. Second, in the RPA the Goldstone modes stemming from the broken symmetries in the mean-field approximation separate exactly [24] from the normal modes.

The decay rate from an initial state i, with spin I_i, to a final state f, with spin I_f, through emission of a photon with multipolarity L and energy E_γ, is given by [25]

$$T_{fi}(E_\gamma) = \frac{8\pi(L+1)}{\hbar L[(2L+1)!!]}\left(\frac{E_\gamma}{\hbar c}\right)^{2L+1} B_{fi}(L) \tag{1}$$

where $B_{fi}(L)$ is the reduced transition probability

$$B_{fi}(L) = \frac{1}{2I_i+1}|\langle f I_f \| \mathcal{M}_L \| i I_i\rangle|^2. \tag{2}$$

The decay rate for a nucleus *at finite temperature* T for emission of a photon of multipolarity L and energy E_γ is obtained from eq. 1 by averaging over the initial states i with fixed spin I_i with the thermal occupation probabilities $p_\mu(I_i)$. Transitions into all states f that have fixed spin I_f and are accessible by energy conservation are allowed:

$$\begin{aligned} T(E_\gamma, I_i \to I_f) &= \sum_{\mu\nu} p_\mu T_{\mu\nu}(E_\gamma)\delta(E_\gamma - [E_\nu(I_f) - E_\mu(I_i)]) \\ &= \frac{8\pi(L+1)}{\hbar L[(2L+1)!!]}\left(\frac{E_\gamma}{\hbar c}\right)^{2L+1} S(E_\gamma, I_i \to I_f), \end{aligned} \tag{3}$$

and

$$S(E_\gamma, I_i \to I_f) = \sum_{\mu\nu} p_\mu \frac{1}{2I_i+1}|\langle \nu(I_f) \| \mathcal{M}_L \| \mu(I_i)\rangle|^2 \delta(E_\gamma - (E_\nu(I_f) - E_\mu(I_i))) \tag{4}$$

is the γ-strength function:

This formula holds in the laboratory system, i.e. with eigenstates of the angular momentum. Writing it in the rotating system requires two changes (see also [23,26]). (i) The axis of quantization must be chosen along the rotation axis. Then, the negative of the m-quantum number of the tensor operator $\mathcal{M}$ coincides with the difference $(I_f - I_i)$. (ii) The energy argument E_γ in the strength function must be shifted by $(I_f - I_i)\omega$, where ω is the cranking frequency (see eq. 11). The result is given by

$$S(E_\gamma, I_i \to I_f) = S_{int}(E_\gamma - \omega(I_f - I_i), I_i \to I_f) \tag{5}$$

with

$$S_{int}(E, I_i \to I_f) = \sum_{\mu\nu} p_\mu \, |\langle \nu(I_f)|Q_{L,I_f-I_i}|\mu(I_i)\rangle|^2 \delta(E - [E_\nu(I_f) - E_\mu(I_i)]) \tag{6}$$

and

$$Q_{L,I_f-I_i} = \sum_m d^L_{I_f-I_i,m}(\frac{\pi}{2})\mathcal{M}^{int}_{Lm} \tag{7}$$

In the special case of a *collective* transition along a rotational band the transition probability is very well described in the FTHFB approach because in this case the decay is a transition between states $|i\rangle$, and $|f\rangle$ of the same intrinsic structure, the $B(E2)$ value can be approximated by

$$\begin{aligned} B(E2, I \to I-2) = S_{int}(E2, I \to I-2) &= \sum_i p_i \, |\langle i|Q_{2-2}|i\rangle|^2 \\ &= |\sum_i p_i \, \langle i|Q_{2-2}|i\rangle|^2 + \sum_m f_m \, (1-f_m) \, (Q^{11}_{2-2})_{mm}. \end{aligned} \tag{8}$$

Here, f_m is the temperature-dependent occupation probability of quasiparticle state m, and Q^{11}_{2-2} is the $\alpha^+\alpha$ part of the operator Q_{2-2} in the quasiparticle representation. In this transition the emitted photon carries two units of angular momentum and an energy $E_\gamma = 2\hbar\omega$, with $\hbar\omega$ the angular frequency defined in eq. 11.

To do a fully microscopic description of the electromagnetic decay we should apply the just mentioned formalism. That means solving the full FTRPA equations at many points of the (E, I) plane. In this paper, however, we are only interested in the description of the collective $E2$ rotational bump obtained after substraction of the statistical gamma rays. Therefore, in order to simplify the calculations, it seems that a good approximation is to evaluate the $B(E2)$ transition probabilities selfconsistently and the statistical ones in the frame of the statistical model. This simplification, on the other hand, will allow us to do a better job in the evaluation of the collective $E2$ transitions. Theories that go beyond the mean field, i.e. theories including fluctuations, take into account, apart from one mean field at a fixed deformation with minimal free energy, further configurations, i.e. at lower excitation energies, in particular, those fields found by changes in the deformation.

At zero temperature the system can execute vibrations in each of these collective parameters (in the case of orientations, where the energy surface is flat in a especific direction, we have rotations). In a microscopic picture these quantum fluctuations can, for instance, be described in the Generator Coordinate Method by a coherent superposition of Slater determinants with different deformations. These fluctuations are expected to decrease very rapidly with increasing excitation energy and are very difficult to evaluate. In our calculation we expect them to play a minor role and will be neglected.

At finite temperatures we have, in addition, statistical -or thermal- fluctuations (in particular in the shape parameter), i.e. the incoherent averaging over many single particle densities based on mean fields with different deformations. According to Landau [27] the probability for a certain value α of the deformation is characterized by the free energy $F(\alpha)$ of the system with this average deformation α

$$p(\alpha) \;\propto\; e^{-F(\alpha)/T}. \tag{9}$$

Using classical statistics, therefore, the probability of emitting a photon with the nucleus having a deformation α between α and $\alpha + d\alpha$ is given by

$$\frac{B(\alpha, E2, I \to I-2) \; e^{-F(I,T,\alpha)/T} D[\alpha]}{\int D[\alpha] \; e^{-F(I,T,\alpha)/T}}, \tag{10}$$

where $B(\alpha, E2, I \rightarrow I-2)$ is the reduced transition probability (see eq. 8) for a system with deformation α and $D[\alpha]$ is the volume element in deformation space. If one takes into account all five quadrupole degrees of freedom $\alpha_{2\mu}$ [11,12], one has $D[\alpha] = \prod_\mu d\alpha_{2\mu} = \beta^4 |\sin 3\gamma| d\beta d\gamma d\Omega$. Often [28,9] one has neglected the fluctuations in the orientation and has averaged only over the deformation parameters β and γ. In this case one has $D[\alpha] = \beta d\beta d\gamma$. In the present calculation we only consider shape fluctuations, we adopt, therefore, the second definition. The energy $E_\gamma(\alpha)$ of the emitted photon is $E_\gamma(\alpha) = 2\hbar\omega(\alpha)$.

For a realistic evaluation of the different observables entering into the electromagnetic decay of a hot nucleus we use the configuration space and the effective interaction of Kumar-Baranger [29] within the frame of the finite temperature Hartree-Fock formalism[1]. In the actual calculations we proceed as follows. First the cranked finite temperature Hartree-Fock equations are solved for fixed temperature and angular momentum by minimizing the grand potential

$$\Omega(I,T) = E - \lambda\, N_0 - \omega\, J - T\, S \tag{11}$$

with the parameters λ and ω determined by the constraints

$$< \hat{N} >= N_0 \qquad < \hat{J}_x >= J = \sqrt{I(I+1)}. \tag{12}$$

with N_0 the proton (neutron) number.

To take into account the fluctuations around the values (β_0, γ_0) of the selfconsistent solution we now minimize the grand potential for constant values of (β, γ). This provide us with surfaces of free energy $F(I,T,\beta,\gamma) = E(T,I,\beta,\gamma) - TS(T,I,\beta,\gamma)$ for fixed values of (T, I). Further details on the calculation can be found in the preceding paper [13]. As mentioned there, a hamiltonian consisting of separable forces, as the effective interaction of Kumar-Baranger [29] used in the present calculations, and without explicit consideration of the Coulomb force, is unable to describe superdeformed shapes. This is an unwanted feature because we know that superdeformed shapes have been measured in these nuclei [30]. Although the decay paths of the nuclei under study do not populate significantly the superdeformed shapes, its absence in our mean field calculation results in insufficient collectivity, particularly in ^{152}Dy. We shall find in our calculations that to obtain quantitative agreement with the experimental data we have to artificially increase the effective quadrupole moment.

III. NUMERICAL SIMULATION.

Let us assume, for the moment, that all the $S(M\lambda)$ are known as a function of the excitation energy and that a cascade calculation or an experiment has been done [31] to determine the entry cloud. To describe the experimental spectra one has to simulate the electromagnetic decay in some way. The cascades are produced in the following way. By a Monte Carlo method we choose a point (E_1, I_1) of the entry cloud; a second Monte Carlo

---

[1]The pairing degrees of freedom are neglected to simplify the computational burden.

decides the energy and multipolarity of the emitted photon, providing us the cooordinates (E_2, I_2) of the next point. The proccess is repeated to provide the energy and multipolarity of the next emitted photon. The gamma rays emitted below a energy cut-off over the yrast line are discarded[2]. The last gamma ray crossing this cut-off is not taken into account. All the emitted photons determine a cascade. In this way we generate several thousand cascades which we can manipulate to produce spectra similar to the experimental ones.

The simulation begins with the calculation of the entry cloud. The average spin of the cloud has the measured value [14,15] and gaussian distribution in spin with width $\sigma(I) = 5\hbar$. The energy dependence of this cloud is somewhat complicated [32]. It is done in a way that reflects the particle emission competition. Essentially, it follows a thermal distribution. The overall effect is not very different from an entry cloud calculated with a rotated blob characterized by two gaussian distributions, one in energy and the other in spin. The energy at which this distribution peaks is chosen to be near the experimentally determined value. The relevant information of the entry points used in the simulation has been collected in Table I.

The transition probabilities for all the decay modes are calculated next. In order to have a simulation that could be compared directly with the experimental data we choose to consider only E1[3] transitions with $(I \rightarrow I-1)$, $(I \rightarrow I)$, and $(I \rightarrow I+1)$ and collective E2 transitions with $(I \rightarrow I-2)$.

The E1 transition probability was calculated using a standard E1 strength function [33], with a Lorentzian shape centered at 14.96 MeV and a width of 5 MeV. Although, in principle, it would have been better to use a shape with two peaks, at least for the well deformed ^{156}Dy, the runs did not show a significant difference. The level density is based on Lang's [34] formula, with $a = A/7$ [14]. Following [35–38], a factor was applied to the strength function to correct the excess of low energy gamma rays and to give a finite limit when $E_\gamma \rightarrow 0$.

The reduced transition probabilities $B(E2)$ are obtained in two different ways: the first one is based on the cranked Finite Temperature Hartree Fock Theory, the second incorporates the shape fluctuations in the way mentioned in the preceding section [4].

The main deficiencies of our model are, probably, the neglect of pairing correlations and the effect, discussed above, that the separable forces used in the calculations do not provide enough softness towards superdeformed shapes. We cannot, therefore expect a quantitative agreement of the experimental and the theoretical average decay path because superdeformed

---

[2]That means discrete lines emitted near the Yrast line are not taken into account.

[3]The E1 was further decomposed into 'statisticals' and 'soil' [14] , the latter determined as those emitted below an energy cut-off.

[4]A third calculation taking into account pairing correlations has been also investigated using the Finite Temperature Hartree Fock Bogoliubov (FTHFB) approximation. One obtains a shift of the spectra to higher energies but not the second bump in ^{154}Dy. The second bump is only obtained when the shape fluctuations are taken into account. A full scale calculation involving both degrees of freedom is very CPU time consuming, and is beyond our possibilities.

shapes are known to exist in ^{152}Dy and neighboring nuclei [30]. Alhassid and Bush [17] have pointed out that the minimum corresponding to superdeformed shapes, which can be quite low in energy at high spin, significantly enhances collectivity since fluctuations cause these highly collective shapes to be sampled. However, as mentioned, we are not able to generate superdeformed shapes with our separable hamiltonian. To mock up the enhancement of collectivity from superdeformed shapes, we have performed some calculations where the operator Q_{2-2} of eq. 8 is artificially increased. In addition, the calculated γ ray energies are also increased to give better agreement with experiment. The increase in energy compensates for the fact that pairing correlations are not included in the calculation. If pairing were included the moment of inertia ($\mathcal{J}$) would be smaller and the cranking frequency larger (in the cranking model $I = \mathcal{J}\omega$ and $E_\gamma = 2\omega$).

These ad hoc enhancements are applied *only in the oblate and transition region* of the (E, I) plane. Specifically we apply the following rules:

- ^{152}Dy. Q_{2-2} is multiplied by 4.0 and the energy of the gamma ray is increased by 0.05 MeV if the spin is greater or equal than $30\hbar$ and the internal excitation energy is greater than 0.2 MeV.
- ^{154}Dy. Q_{2-2} is multiplied by 2.5 and the energy of the gamma ray is increased by 0.15 MeV if the spin is greater or equal than $34\hbar$ and the internal excitation energy is greater than 0.2 MeV.
- ^{156}Dy. Q_{2-2} is multiplied by 1.22 and the energy of the gamma ray is increased by 0.225 MeV if the spin is greater or equal than $44\hbar$ and the internal excitation energy is greater than 0.2 MeV.

The fact that we use smaller factors with increasing mass number is consistent with the experimental finding that the superdeformed have been populated in Dy isotopes with $A = 152$ and 153 and not in those with larger A. We want to emphasize, however, that the calculations with these additional procedures do not provide new physics but a better quantitative agreement with the experimental results. They indicate that, despite the inclusion of fluctuations, there is an overall deficiency of collectivity. In Table II we show the multiplicities and spin exit points obtained in the different calculations. Experimental results are given in table III for comparison.

The quasicontinuum cascades are terminated for U below 1.5 MeV for ^{152}Dy, 1.0 MeV for ^{154}Dy, and 0.7 Mev for ^{156}Dy following refs. [14,15].

IV. RESULTS

The experimental results [14,15] which we are attempting to reproduce are depicted in figs. 1 and 2 (dashed lines). These spectra were obtained by populating high-spin states of ^{152}Dy, ^{154}Dy and ^{156}Dy via the reaction ^{120,122,124}Sn(^{36}S,$4n$)$^{152-154-156}$Dy with 148-165 MeV beams from ATLAS (Argonne Tandem Linac Accelerator System). For the nucleus ^{154}Dy data were obtained with three bombarding energies (148, 155, and 165 MeV) to vary the angular momentum of the entry distribution. The experimental espectra for the low, medium and high angular momentum distribution, shown by the dashed lines in fig. 2, are

of the quasicontinuum collective E2 γ-rays emitted from highly excited states. Broad E2 peaks were obtained in all three Dy isotopes. Only single components could be discerned in ^{152,156}Dy (fig. 1), but two distinct peaks were seen in ^{154}Dy, particularly at the highest beam energy (fig. 2).

The spectra obtained by our calculations are compared with the experimental ones in Figs. 1 and 2. The spectra for ^{152}Dy and ^{156}Dy are shown in Fig. 1. The left panel shows results using the FTHF theory, i.e. mean field approximation with no fluctuations. For ^{152}Dy, no E2 γ-rays are obtained since the quasicontinuum cascades all occur in the region where the nucleus is oblate. In contrast, all cascades in ^{156}Dy occur in the domain where the nucleus is collective, so that a pronounced E2 peak is obtained (although at lower energy than measured).

These features can be clearly seen by looking at Fig. 3 where we have represented contour lines of the (β, γ) deformations as a function of the excitation energy and the angular momentum, together with several cascades of the theoretical simulation. In Fig. 3 we see in the lower part, for ^{156}Dy, that most of the cascade go through a region corresponding to a well deformed prolate nucleus. This picture agrees with the spectrum observed in Fig. 1. In the upper part we observe that the cascades of the nucleus ^{152}Dy flow along a path corresponding to a slightly deformed oblate nucleus. This is reflected in the left panel of Fig. 1 in the absence of an $E2$ peak.

The middle panels of fig. 1 gives the results when shape fluctuations are included. An immediate consequence is that the collective region of the $\beta-\gamma$ plane is now sampled through the fluctuations. Thus, a quasicontinuum E2 peak is now present in ^{152}Dy. However, the peak is still smaller that the experimental one, showing that there is still insufficient collectivity. Inclusion of fluctuations smooths out the E2 spectrum in ^{156}Dy, but otherwise the overall spectral shape is not changed since collectivity was already present without fluctuations.

The right panels in fig. 1 show spectra from calculations where the ad hoc procedure is introduced to increase Q_{2-2} and E_γ. As discussed above, the increase of Q_{2-2} compensates for the insufficient collectivity, due to the absence of a superdeformed minimum which is known to occur at high spin [30] and which would otherwise have been sampled by the fluctuations [17]. The increase in E_γ compensates for the neglect of pairing, which would have increased the transition energies by decreasing the moment of inertia. With the ad hoc procedure introduced to overcome deficiencies in the mean-field part of the theory, excellent agreement is obtained with experiment for both ^{152,156}Dy. However, this is hardly surprising since the procedure was tuned to produce agreement.

Fig. 2 shows the results for ^{154}Dy. In the left panels, where no fluctuations are included, only the portion of the cascade in the collective region gives rise to a E2 peak, as in ^{156}Dy. The portion which is in the oblate region does not yield a E2 component, as in ^{152}Dy. This can be seen in fig. 4 where we have the same plots as in Fig. 3 but for the three entry points of the nucleus ^{154}Dy. In the low entry point plot most of the cascade go through a region of prolate deformation, thus generating the one bump structure observed in the left panel of fig. 2. At medium and high energy entry points, a fraction of the cascades start in a region of medium triaxial deformation. The admixture of this fraction is responsible for the appearance of some high energy (> 1 MeV) γ-rays, mainly at the high bombarding energy in the left panel of fig. 2.

The situation improves when fluctuations are included (middle panels); the part of the

cascade in the oblate region can now give rise to the high-energy E2 peak, again as observed for ^{152}Dy. For the low entry spin conditions corresponding to the lowest beam energy, most of the cascade are in the collective region, so that no noticeable high-energy component appears. For conditions appropriate for the middle beam energy, a few cascades are present in the oblate region, giving rise to a small high-energy shoulder. At the highest beam energy, sufficient angular momentum is brought in to give significant cascades in the oblate region, thereby yielding a distinct high-energy peak. The spectrum for ^{154}Dy can be viewed as a superposition of contributions from ^{152,156}Dy, or from cascades in the regions where the nucleus is either oblate (non-collective) or collective. Although the overall multiplicity is smaller than measured (due to insufficient collectivity), the distinct two-peak feature observed experimentally is reproduced. This is a manifestation that cascades from both the oblate and collective regions on either side of the predicted phase boundary now contribute to the E2 spectrum. Hence the two-peak feature is a signature that the phase transition present in the mean-field theory is not washed out completly by the fluctuations. Indeed the fluctuations are responsible for the high-energy peak. The right panels shows that inclusion of ad hoc procedures to compensate for deficiencies in the mean-field theory yield very good agreement with experiment.

V. CONCLUSIONS

We have performed a study of the electromagnetic decay of three nuclei at different entry points to analyze the collective $E2$ espectra. In the numerical simulations we have incorporated a microscopic calculation of the collective $E2$ transition probabilities. For the statistical $E1$ we use the statistical model prescription, with the $E1$ γ strength function proposed in ref. [35]. We obtain a reasonable agreement with the experimental results only by inclusion of the fluctuations associated with the shape degrees of freedom. This is a clear cut demonstration of the vital role of fluctuations in the collective properties of nuclei.

We found that the two-bump structure of ^{154}Dy (at the highest beam energy) is caused by a phase transition from a prolate well deformed nucleus at low angular momentum to an oblate deformed one at high angular momentum. Thus, despite the fluctuations present in a finite system, signs of a phase transition are seen to persist.

In conclusion, we have implemented for the first time theoretical $B(E2)$'s in cascade codes describing the decay of highly excited nuclei. We find a qualitative agreement with the experimental date and we believe that this a significant achievement. This should encourage calculations along the lines of this paper which also incorporate full microscopic strengh functions for all decays, as proposed in ref. [22,23].

ACKNOWLEDGMENTS

We (V.M. and J.L.E.) would like to thank the staff at the computing facility at the Facultad de Informatica of the Universidad Politécnica de Madrid for their technical support.

This work was partially supported by DGICyT, Spain under project PB91-0006 and by the U.S Dept. of Energy, Nuclear Physics Division, under contract W-31-109-ENG-38.

REFERENCES

[1] A.L. Goodman *Adv. Nucl. Phys.* vol. **11**, Eds. J. Negele and E. Voigt (Plenum, New York 1979)
[2] J.L. Egido, H.J. Mang and P. Ring *Nucl. Phys.* **A339**, 390 (1980).
[3] A.L. Goodman *Nucl. Phys.* **A369** (1981) 365; **A370**, 90 (1981).
[4] K. Sugawara-Tanabe, K. Tanabe and H.J. Mang *Nucl. Phys.* **A357**, 20, 45 (1981).
[5] J.L. Egido, P. Ring and H.J. Mang *Nucl. Phys.* **A451**, 77 (1986).
[6] L. G. Moretto *Phys. Lett* **44**, 494 (1973).
[7] A.L. Goodman *Phys. Rev.* **C29**, 1887 (1984).
[8] J. L. Egido, P. Ring, S. Iwasaki and H. J. Mang *Phys. Lett.* **154B**, 1 (1985).
[9] J.L. Egido, C. Dorso, J.O. Rasmussen and P. Ring *Phys. Lett.* **178B**, 139 (1986).
[10] A.L. Goodman, Phys. Rev. **39**, 2478 (1989).
[11] Y. Alhassid, B. Bush and S. Levit *Phys. Rev. Lett.* **61**, 1929 (1988).
[12] Y. Alhassid and B. Bush *Nucl. Phys.* **A509**, 461 (1990).
[13] V. Martin and J. L. Egido, Phys. Rev. C (previous paper)
[14] R. Holzmann *et al. Phys. Lett. B* **195**, 321 (1987).
[15] R. Holzmann *et al. Phys. Rev. Lett. B* **62,** 520 (1989).
[16] A.L. Goodman, Nucl. Phys. **A504**, 413 (1989).
[17] Y. Alhassid in "New trends in Nuclear Collective Dynamics", Springer Proccedings in Physics, vol. 58, Y. Abe, H. Horiuchi and K. Matsuyanagi eds., Springer Verlag, New York 1991, p 41-90.
[18] J. L. Egido and P. Ring *J. Phys. G* **19**, 1 (1993).
[19] R.J. Liotta and R.A. Sorensen *Nucl. Phys.* **A297**, 136 (1978).
[20] G. Leander, Y.S. Chen and B.S. Nilsson *Phys. Ser.* **24**, 164 (1981).
[21] M. Wakai and A. Faessler *Nucl. Phys.* **A307**, 349 (1978).
[22] J.L. Egido and H.A. Weidenmüller *Phys. Lett.* **208**, 58 (1988).
[23] J.L. Egido and H.A. Weidenmüller *Phys. Rev.* **C39**, 2398 (1989).
[24] J.L. Egido and J.O. Rasmussen *Nucl. Phys.* **A476**, 48 (1988).
[25] A. Bohr and B.R. Mottelson *Nuclear Structure*, Vol. II (Benjamin, Reading, Mass. 1975)
[26] P. Ring, L.M. Robledo, J.L. Egido and M. Faber *Nucl. Phys.* **A419**, 261 (1984).
[27] L.D. Landau and E.M. Lifshitz *Course of Theoretical Physics* (Pergamon Press, Oxford 1959)
[28] M. Gallardo, M. Diebel, T. Dossing and R.A. Broglia *Nucl. Phys.* **A443**, 415 (1985).
[29] K. Kumar and M. Baranger, Nucl. Phys. **A110**, 529 (1968)
[30] P. Twin and P. Nolan *Ann. Rev. Nucl. Part. Sc.* vol. **38**, 533 (1988).
[31] F. Puhlhofer *Nucl. Phys.* **A280,** 267 (1977).
[32] G.A. Leander. *Comp. Phys. Comm.* **47,** 311 (1987).
[33] G.A. Bartholomew *et al. Adv. Nucl. Phys.* **17,** 229 (1973).
[34] D.W. Lang. *Nucl. Phys.* **77,** 545 (1966).
[35] S.G. Kadmenskii *et al. Sov. J. Nucl. Phys.* **37**(2), 165 (1983).
[36] C. M. McCullagh, M. L. Stelts, R.E. Chrien *Phys. Rev. C* **23**, 1394 (1981).
[37] G. A. Leander *Phys. Rev. C* **38**, 728 (1988).
[38] J. Kopecky, M. Uhl *Phys. Rev. C* **41**, 1941 (1990).

TABLES

TABLE I. Entry points used in the simulation.

Nucleus	$< I >$	$< E >$	$< E_{exp.} >$
^{152}Dy	46.7	24.0	25.6
^{154}Dy	50.2	25.0	26.9
^{154}Dy	42.7	20.0	22.0
^{154}Dy	35.9	16.5	18.0
^{156}Dy	48.8	24.0	25.4

TABLE II. Multiplicities and exit spins for the four different cases, mean field, mean field plus shape fluctuations, mean field with artificial enhancement and mean field plus shape fluctuations with artificial enhancement.

	Mean Field			Mean Field Plus Shape Fluctuations		
Nucleus	E2 Mult.	E1 Mult.	$< I > \pm\sigma$	E2 Mult.	E1 Mult.	$< I > \pm\sigma$
^{152}Dy	0.001	3.915	43.7±5	1.207	3.870	41.5±5
^{154}Dy	5.19	5.292	45.0±7	5.097	4.873	41.9±6
^{154}Dy	4.178	4.5	37.2±7	3.697	4.279	36.3±6
^{154}Dy	2.777	4.371	30.8±6	2.496	4.282	30.6±5
^{156}Dy	9.142	5.916	33.6±8	9.556	5.601	33.6±9
	With enhanced BE2 and E_γ					
^{152}Dy	0.002	3.915	43.4±5	4.809	3.799	35.0±6
^{154}Dy	7.328	4.691	40.4±11	8.606	4.173	33.5±9
^{154}Dy	6.56	4.091	30.8±9	5.996	3.802	30.3±7
^{154}Dy	4.41	4.102	26.2±6	3.973	4.007	26.5±6
^{156}Dy	11.69	4.136	24.2±10	10.376	3.699	25.9±11

TABLE III. Experimental results obtained from [14,15]

	^{152}Dy	^{154}Dy	^{154}Dy	^{154}Dy	^{156}Dy
E_{beam} (MeV)	160	165	155	148	155
$< I_{entry} > (\hbar)$	46.7	50.2	42.7	35.9	48.8
$< E_{entry} >$ (MeV)	25.6	26.9	22	18	25.4
$< I_{exit} > (\hbar)$	34.1	30.0	25.1	21.2	26.3
$< M_{quad.} >$	5.3	9.1	7.8	6.4	10.3

FIGURES

FIG. 1. Quasicontinuum $E2$ γ-spectra for the ^{152}Dy and ^{156}Dy nuclei at a beam energy of 160 MeV for ^{152}Dy and 155 MeV for ^{156}Dy (experimental results in dashed lines) and three type of calculations (solid lines) in the three columns (FTHF, FTHF plus shape fluctuations, SF, and FTHF+SF with artificial enhancements in the oblate region, respectively).

FIG. 2. Same as fig. 1 for ^{154}Dy at three different beam energies (top panel 165 MeV, middle 155 MeV and bottom panel row 148 MeV).

FIG. 3. Energy versus angular momentum for the nuclei ^{152}Dy and ^{156}Dy at their corresponding entry points. The solid lines above the yrast line are contour lines of beta deformation, the dashed ones are the contour lines of constant gamma deformation values; these values have been obtained from the FTHFB calculations of the preceding paper [13]. The dashed line parallel to the yrast line corresponds to the energy cut-off used to eliminate the discrete lines. The line ($\gamma = -60°$) separates the collective and oblate states. The region above this phase boundary corresponds to oblate aligned particle motion. The arrows represent several decay cascades given by the simulation. The simulation corresponds to the calculations including shape fluctuations.

FIG. 4. Same as figure 3 for the ^{154}Dy nucleus starting at the three different entry points.

Fig. 1

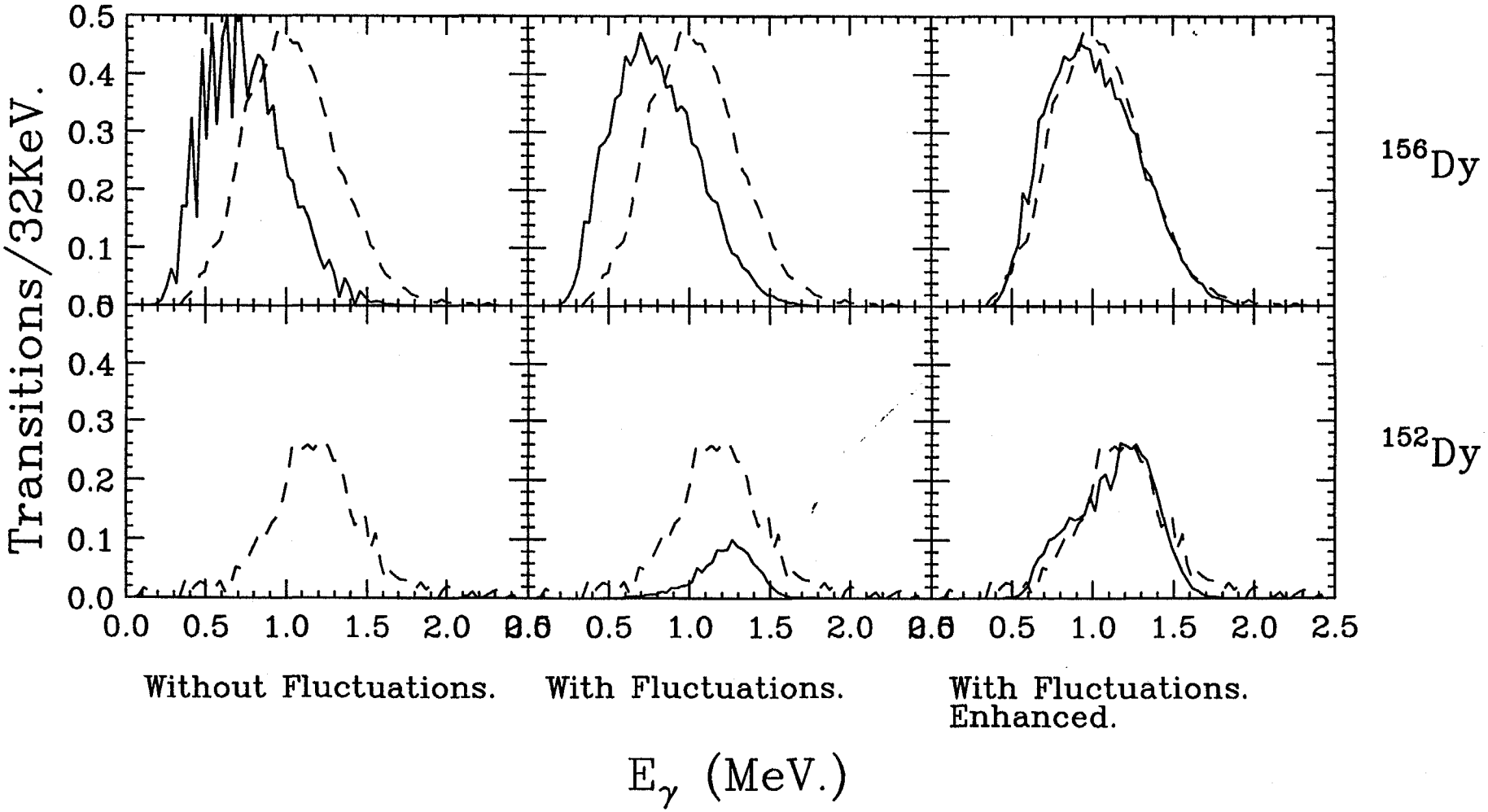
Transitions/32KeV.
0.5
0.4
0.3
0.2
0.1
0.0
0.0 0.5 1.0 1.5 2.0 2.5
^{156}Dy
^{152}Dy
Without Fluctuations.
With Fluctuations.
With Fluctuations.
Enhanced.
E_γ (MeV.)

Fig. 2

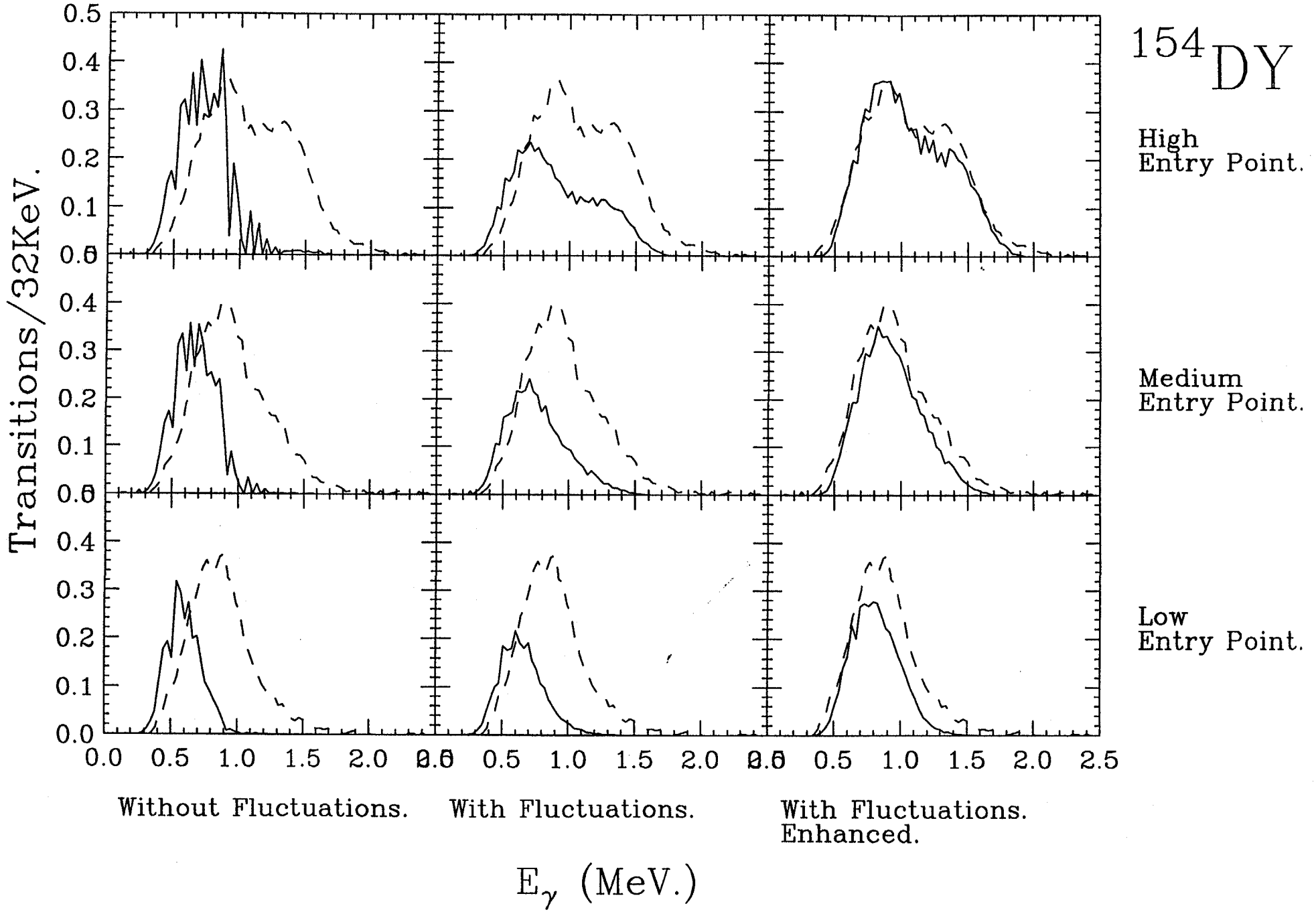
154DY
High Entry Point.
Medium Entry Point.
Low Entry Point.
Transitions/32KeV.
0.0
0.1
0.2
0.3
0.4
0.5
0.0 0.5 1.0 1.5 2.0 2.5
Without Fluctuations.
With Fluctuations.
With Fluctuations. Enhanced.
E_γ (MeV.)

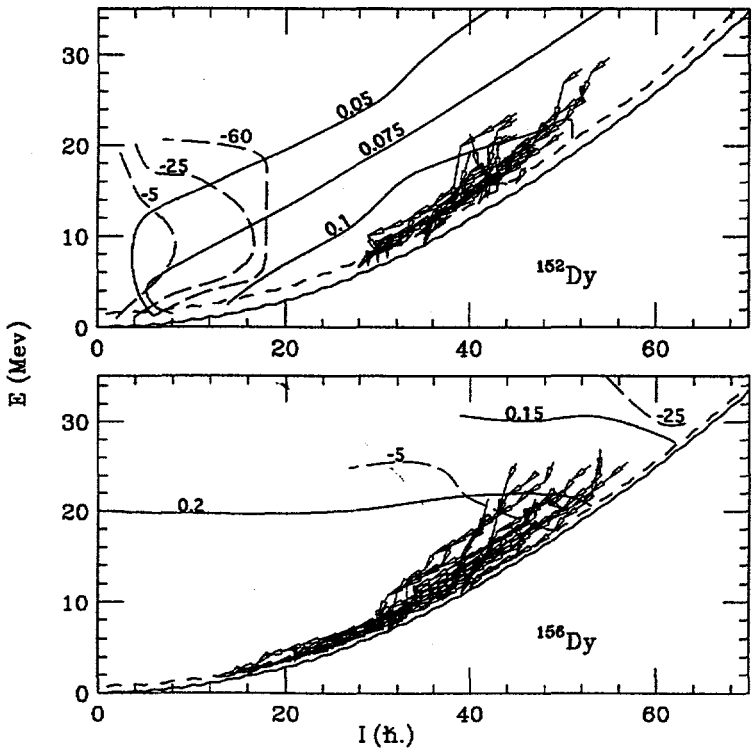

Fig. 3

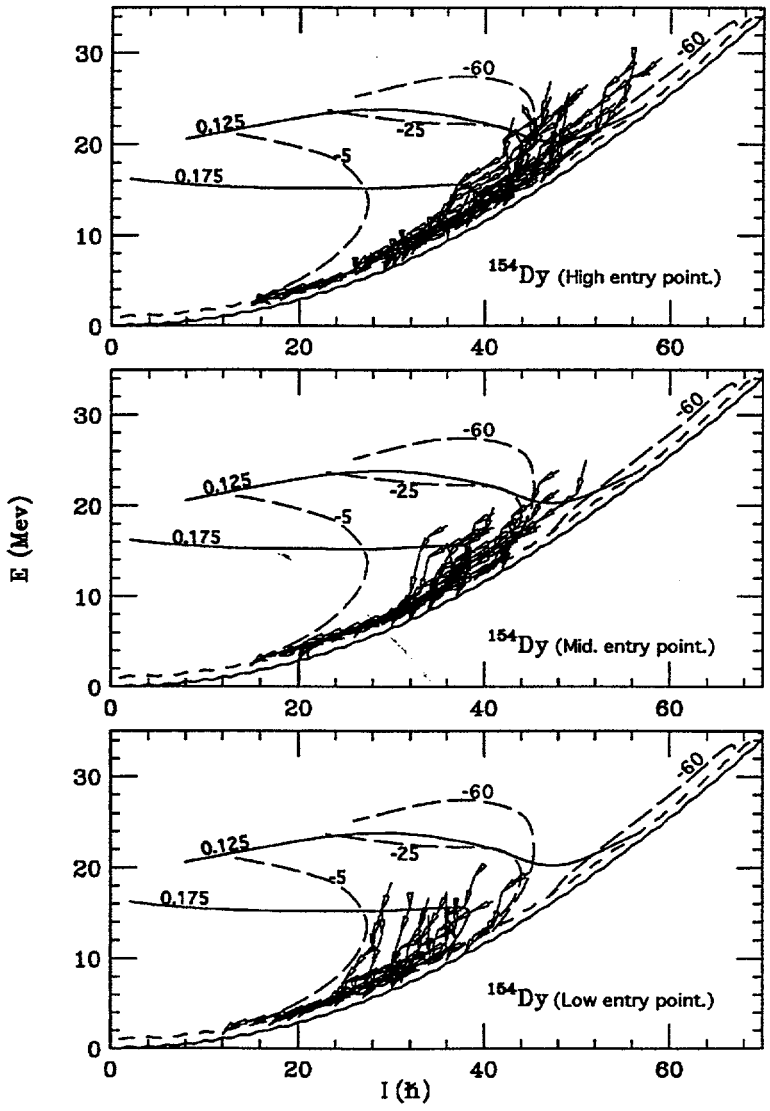
E (Mev)
I (ħ)
-60
-25
-5
0.125
0.175
^{154}Dy (High entry point.)
^{154}Dy (Mid. entry point.)
^{154}Dy (Low entry point.)

Fig. 4